

Back-Skip of the Growing Chain at Model Complexes for the Metallocene Polymerization Catalysis

Gaetano Guerra,* Luigi Cavallo, Gilberto Moscardi, Michele Vacatello, and Paolo Corradini

Dipartimento di Chimica, Università di Napoli, Via Mezzocannone 4, I-80134 Napoli, Italy

Received November 27, 1995; Revised Manuscript Received March 4, 1996[®]

ABSTRACT: A molecular mechanics analysis on model metallocene complexes, as possible intermediates for the propene polymerization, in which the two coordination positions available for the monomer and the growing chain are diastereotopic, is presented. The energy difference between the corresponding diastereoisomeric preinsertion intermediates appears to be relevant for the model complexes based on the *meso*-ethylenebis(4,5,6,7-tetrahydro-1-indenyl) ligand (**1**), the isopropylidene[(3-methyl(η^5 -cyclopentadienyl))(η^5 -9-fluorenyl)] ligand (**2**), and the *rac*-ethylene[1-(η^5 -9-fluorenyl)-1-phenyl-2-(η^5 -1-indenyl)] ligand (**3**), while it appears to be small for those based on the *rac*-ethylene[1-(η^5 -cyclopentadienyl)-1-phenyl-2-(η^5 -1-indenyl)] ligand (**4**). It is suggested that these energy differences can be related to an increased probability of a back-skip of the growing chain toward the outward coordination position after the monomer insertion and prior to the coordination of a new olefin molecule. The kinetic competition between the back-skip of the chain outwards and the monomer coordination is able to rationalize the kinds of defects in prevalently hemi-isotactic chains obtained with systems based on **3**, as well as the increased stereoregularity at decreasing monomer concentration for systems based on **3** (not shown by systems based on **4**). The molecular mechanics analysis shows that the nonbonded interactions are also able to account for the influence of the ethylene bridge conformation on the stereospecificity of the propene polymerization in *ansa*-zirconocene complexes.

Introduction

The mechanism for the Ziegler–Natta polymerization of the olefins, proposed by Cossee^{1,2} several years ago, consists of two consecutive steps: coordination of the olefin to the catalytic center and insertion into the metal–carbon bond through a *cis*-opening.^{2–4} This mechanism assumes that, in the insertion step, there is a migration of the growing chain to the position previously occupied by the coordinated monomer (chain migratory insertion). In the following, we will distinguish as “alkene-free” and “alkene-bound” the two possible states of the metal atom, constituting the catalytic center which may have, thus, different degrees of coordinative saturation.

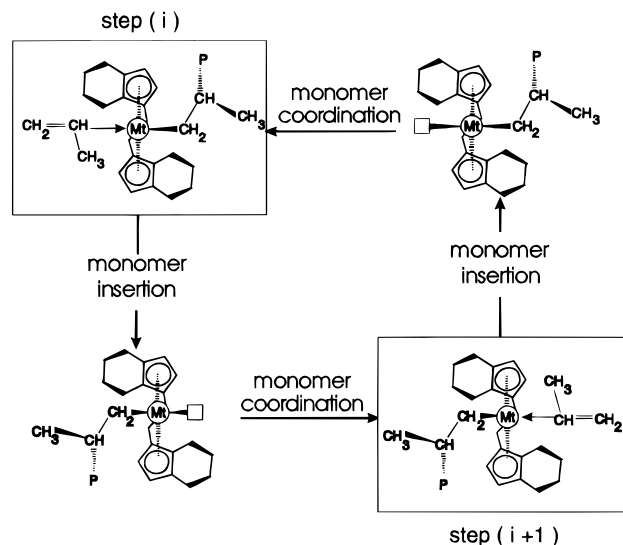
In the framework of the chain migratory insertion mechanism, the stereospecificity of the model catalytic center depends on the enantioselectivities of the insertion steps, which correspond to the two alkene-bound intermediates obtained by exchanging the relative positions of the growing chain and the incoming monomer. Depending on the structure of the model catalytic center, these two alkene-bound intermediates can be of the following type.

(i) Identical, when the two available coordination positions are homotopic.⁵ These model centers, if the insertion step is enantioselective, are consequently isospecific. Model catalytic centers presenting a C_2 -symmetry axis, which locally relates the atoms which are relevant to the nonbonded interactions with the monomer and the growing chain, were proposed by Allegra several years ago for the heterogeneous catalysis on TiCl_3 .⁶ Analogous models with C_2 -symmetry axes, relating the atoms of the stereorigid ligand, have been more recently proposed^{7–9} for the new homogeneous isospecific Ziegler–Natta catalysts based on metallocenes^{9–11} (Scheme 1).

* Address for correspondence: Dipartimento di Chimica, Università di Salerno, I-84081 Baronissi (SA), Italy.

[®] Abstract published in *Advance ACS Abstracts*, May 1, 1996.

Scheme 1



(ii) Enantiomeric, when the two available coordination positions are enantiotopic.⁵ These model catalytic centers, if the insertion step is enantioselective, are consequently syndiospecific. Model catalytic centers with a C_s -symmetry plane, relating the atoms of the stereorigid ligand, have been proposed^{12,13} to account for the obtaining of syndiotactic polyolefins with other metallocene-based catalysts.^{9,12}

(iii) Diastereoisomeric, when the two available coordination positions are nonequivalent (diastereotopic)⁵ but of similar energy. In the hypothesis that the chain migratory insertion mechanism (Figure 1) is still prevailing, these model catalytic centers would be isospecific or syndiospecific if these two situations present the same or an opposite kind of enantioselectivity and hemi-isospecific if only one of the two situations is enantioselective. Models of this kind have been proposed in order to rationalize the obtaining of the hemi-isospecific polypropylene^{13,14} with a homogeneous metallocene

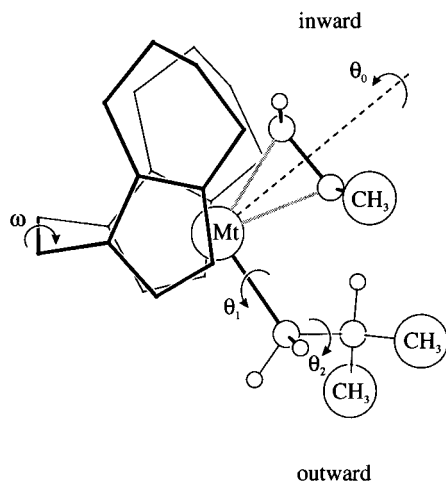


Figure 1. Schematic drawing of a model of a preinsertion intermediate including the *meso*-ethylenebis(η^5 -tetrahydroindenyl) ligand with an inward *si*-propene coordination. The main internal coordinates which have been varied in the calculations are indicated. The sketched conformation corresponds to $\theta_0 = 0^\circ$, $\theta_1 = -60^\circ$, $\theta_2 = +40^\circ$, and $\omega = 45^\circ$ (δ conformer) (see text).

catalyst based on the isopropylidene[(3-methyl(η^5 -cyclopentadienyl))(η^5 -9-fluorenyl)] ligand.⁹

(iv) Diastereoisomeric but of substantially different energy. For these model catalytic centers, the polymerization mechanism could be altered; the growing chain in successive coordination steps could occupy always the same coordination position, that is, after each migratory insertion step (in the alkene-free state), it could move back to the previous coordination position (back-skip of the growing chain).

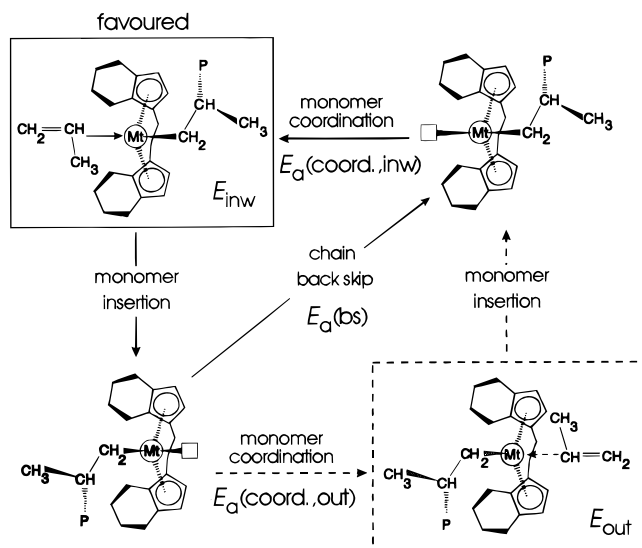
It is worth noting that the characterization of the stereosequences in polymers obtained by well-characterized metallocene complexes has produced a general acceptance of the chain migratory insertion mechanism and of models of the kind i–iii. On the contrary, at the moment, no conclusive experimental evidence supports the occurrence, for any catalytic system, of a polymerization mechanism with a regular back-skip of the chain.

The model sites proposed by Cossee,¹ for the heterogeneous isospecific polymerization, located on lateral surfaces of α - TiCl_3 were of the kind iv. Since only the lower energy diastereoisomeric situation would be enantioselective,^{1,15} these model sites imply, for their isospecificity, a regular back-skip of the growing chain. Analogous model sites, but on layers in relief with respect to lateral faces of layered TiCl_3 structures,^{15–17} as well as for TiCl_4 supported on MgCl_2 ,¹⁸ were considered in the molecular mechanics studies conducted several years ago in our group.

Recently, also for homogeneous catalysts, the possibility of a back-skip of the growing chain, in the alkene-free state, has been invoked in order to rationalize the behavior of the catalytic systems based on the *meso*-ethylenebis(4,5,6,7-tetrahydro-1-indenyl) ligand¹⁹ (Scheme 2) and the *rac*-ethylene[1-(η^5 -9-fluorenyl)-2-(η^5 -1-indenyl)] ligand, bearing a variable bridge substitution pattern.²⁰ Moreover, the occurrence of occasional back-skips of the chain (skipped insertions) has been invoked to interpret some of the stereochemical defects in the syndiotactic and hemi-isotactic polypropylenes.^{9,12,14}

The application by some of us of simple molecular mechanics techniques to preinsertion intermediates (alkene-bound intermediates in a conformation near the transition state for the monomer insertion) for the

Scheme 2

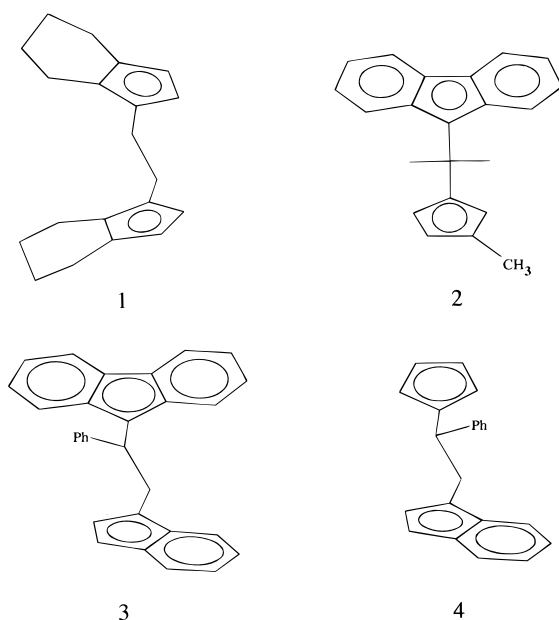


heterogeneous^{15–18} and (both isospecific^{7,8,21} and syndiospecific¹³) homogeneous Ziegler–Natta polymerizations has allowed to highlight a common mechanism of enantioselectivity which involves a chiral orientation of the growing chain.^{7,15,21} This mechanism is in agreement with several experimental facts and is strongly supported by the results obtained by Zambelli and co-workers,^{22,23} relative to the enantioselectivities in the initiation steps, in the presence of different alkyl groups. This mechanism of enantioselectivity has been also confirmed by other computational studies involving also the modeling of possible transition states of the monomer insertion reaction.^{24–27}

In particular, models for catalytic systems with *rac*-ethylenebis(4,5,6,7-tetrahydro-1-indenyl) and *rac*-ethylenebis(1-indenyl) ligands were deeply studied by molecular mechanics techniques.^{7,21,25,27} These models are able to rationalize the observed enantioselectivities, not only for the regioregular placements but also for the regioirregular placements.²¹ Moreover, the nonbonded interactions in the models have been shown to give a contribution to the regiospecificity in favor of the primary insertion, even after an occasional secondary insertion, as well as to the higher regiospecificity observed for titanocene-based, with respect to zirconocene-based, catalytic systems.²¹

The good predictive ability of this kind of molecular mechanics analysis encouraged us to evaluate, for unsymmetric metallocene complexes, the energy differences $E_{\text{out}} - E_{\text{inw}} = \Delta E$, see Scheme 2, between the preinsertion intermediates of the two diastereoisomeric alkene-bound intermediates, obtained by exchanging the relative positions of the growing chain and the incoming monomer. Of course, the probability of occurrence of a back-skip of the chain, in the alkene-free state, is only indirectly dependent on ΔE . It is, in fact, dependent on the difference between the activation energy for the chain back-skip ($E_a(\text{bs})$ in Scheme 2) and the activation energy for the formation of the high-energy alkene-bound intermediate ($E_a(\text{coord.,out})$ in Scheme 2). However, since the degree to which empirical force fields can be used for prediction of transition states is not well established²⁸ and since the activation energy $E_a(\text{coord.,out})$ is expected to increase with increasing E_{out} , for the sake of simplicity, in this paper, we confine our molecular mechanics analysis to the energies of the diastereoisomeric alkene-bound intermediates.

Chart 1



In particular, in the first and the second sections, models of alkene-bound intermediates including a *meso*-ethylenebis(4,5,6,7-tetrahydro-1-indenyl) ligand (**1**) or an isopropylidene[(3-methyl(η^5 -cyclopentadienyl))(η^5 -9-fluorenyl)] ligand (**2**), respectively, are considered.

In the third section, the model alkene-bound intermediates for the diastereoisomeric complexes, with different bridge conformations (δ or λ), based on the ethylene[1-(η^5 -9-fluorenyl)-1-phenyl-2-(η^5 -1-indenyl)] ligand (**3**) (whose separation and characterization have been recently described by Rieger et al.²⁰) are considered. The corresponding catalytic systems show substantial increments of the isospecificity with decreasing monomer concentration, suggesting the occurrence, for low monomer concentrations, of the phenomenon of the back-skip of the chain.²⁰

In the fourth section, an analogous analysis for the diastereoisomeric complexes, based on the ethylene[1-(η^5 -cyclopentadienyl)-1-phenyl-2-(η^5 -1-indenyl)] ligand (**4**), is presented. According to the study of Rieger et al., the corresponding catalytic systems do not show any increment of the isospecificity with decreasing the monomer concentration, suggesting the substantial absence of the phenomenon of the back-skip of the chain.²⁰

The calculations of the third and fourth sections are also aimed to assess the ability of the models and the proposed enantioselectivity mechanism (of the chiral orientation of the growing chain) to account for the observed differences in the stereospecific behavior between diastereoisomeric complexes with different bridge conformations.²⁰

Models

As in previous papers,^{7,8,13,21} the basic models of the alkene-bound intermediates considered in this paper are metal complexes containing three ligands, which are a π -coordinated propene molecule, a σ -coordinated isobutyl (simulating a primary growing chain), and a stereorigid π -coordinated ligand (**1–4**).

We recall the definitions of the most important internal coordinates which have been varied (see Figure 1): the dihedral angle θ_0 associated with rotations of the olefin around the axis connecting the metal to the center of the double bond, the internal rotation angles

θ_1 and θ_2 associated with rotations around the bond between the metal atom and the first carbon atom of the growing chain and between the first and the second carbon atom of the growing chain, respectively, and the dihedral angle ω associated to the ethylene bridge conformation for **1**, **3**, and **4**. At θ_0 near to 0° the olefin is oriented in a way suitable for primary insertion, while θ_0 near to 180° corresponds to an orientation suitable for secondary insertion. θ_1 near to 0° corresponds to the conformation having the first C–C bond of the growing chain eclipsed with respect to the axis connecting the metal atom to the center of the double bond of the olefin. $\theta_2 = 0^\circ$ corresponds to the conformation with the Mt–C(chain) bond eclipsed with respect to the C–H bond of the second carbon atom of the chain. The ω values relative to the energy minima are close to 45° or -45° , and the corresponding conformations are referred in the following as δ and λ ,^{20,29,30} respectively.

A prochiral olefin such as propene may give rise to nonsuperposable coordinations, which can be labeled with the notations *re* and *si*.³¹ The coordination of the ligands **2–4** is chiral, and can be labeled with the notation *R* or *S* according to the rules of Cahn–Ingold–Prelog³² extended to chiral metallocenes as outlined by Schlögl.³³ The symbols *R* and *S* indicate the absolute configuration of the bridgehead carbon atom of the 3-methylcyclopentadienyl group, for ligand **2**, and of the indenyl groups, for ligands **3** and **4**, respectively. Without loss of generality, all the reported calculations refer to the *R* coordination of ligands **2–4**.

For all the considered pseudotetrahedral alkene-bound intermediates, an intrinsic chirality at the central metal atom is present, which can be labeled with the notation *R* or *S*, by an extension of the Cahn–Ingold–Prelog rules, as proposed by Stanley and Baird.³⁴ This nomenclature has been used by us to distinguish the diastereoisomeric alkene-bound intermediates which may arise by exchanging the relative positions of the growing chain and the incoming monomer.¹³ However, in this paper we will mainly use the more mnemonic indication according to which the relative disposition of the ligands, which presents the coordinated monomer in the more (less) crowded region, is referred to as “inward (outward) propene coordination”.

We also recall that, in the framework of our analysis, the conformations of alkene-bound intermediates are considered sufficiently close to the transition state and considered as suitable conformers of preinsertion intermediates, only if the insertion can occur through a process of “least nuclear motion”.^{1,35–37} This corresponds to geometries of the alkene-bound intermediates for which (i) the double bond of the olefin is nearly parallel to the bond between the metal atom and the growing chain ($\theta_0 \approx 0^\circ$ or $\theta_0 \approx 180^\circ$) and (ii) the first C–C bond of the chain is nearly perpendicular to the plane defined by the double bond of the monomer and the metal atom ($|\theta_1| \approx 60\text{--}90^\circ$ rather than $\theta_1 \approx 180^\circ$).^{37a} Let us recall that θ_1 values away from 180° and near to 60° are also suited for the formation of an α -agostic bond, which has been shown to stabilize the transition state for the insertion step in some scandium- and zirconium-based catalysts.^{38–40}

Moreover, alkene-bound intermediates for which the methyl group of the propene and the second carbon atom (and its substituents) of the growing chain are on the same side with respect to the plane defined by the Mt–C bonds ($\theta_1 \approx 60^\circ$ and -60° for the *re*- and *si*-coordinated monomers, respectively) are assumed to be unsuitable for the successive monomer insertion. In fact, the insertion paths starting from these intermediates in-

volve large nonbonded interactions.^{15,18,21} We assume that the energy differences between suitable preinsertion intermediates are close to those present in the corresponding transition states for the insertion reaction.

Calculation Method

In the molecular mechanics calculations presented in this paper, contributions to the energy relative to the angle bendings, "out-of-plane bendings", torsional barriers to internal rotations, and nonbonded interactions have been included. Bond lengths have been instead kept constant: This assumption is reasonable in the neighborhood of the energetic minima corresponding to the geometry of not overcrowded molecules.

As in previous papers,^{8,13,21} a harmonic potential has been used in order to evaluate the bending contribution to the total energy of the X-C_t-X angles (where C_t stands for tetrahedral carbon and X ≡ C_t or H); the bending parameters have been taken from ref 41. The parameters for the Mt-C_t-C_t and Mt-C_t-H angles have been arbitrarily assumed to be equal to those for the C_t-C_t-C_t and C_t-C_t-H angles, respectively.

With respect to previous calculations,^{8,13,21} the difference is that the coordination of the bridged π-ligand is less rigid: The bond between the metal and a dummy atom placed at the center of the five-membered rings (D_π), as well as the angles Mt-D_π-C_π (where C_π stands for carbon atom of the π-ligands) and D_π-Mt-D_π, are given equilibrium values and stretching and bending force constants, respectively, as described by Bosnich in ref 42; as in previous papers,^{19,21} the bending parameters for the angles D_π-Mt-C_t and D_π-Mt-D_{ol} (where D_{ol} is a dummy atom placed at the center of the double bond of the π-coordinated olefin) are taken to be equal to those for the H-C_t-H angle; finally, as previously,^{8,13,21} the angle C_t-Mt-D_{ol} has been restrained in the experimentally observed range 91–99°. ³⁰

For the bridging carbon atoms and the methyl group of the ligand **2**, a bending potential for the C_π-C_π-C_t angle is taken from ref 42, and an energy term for an "out-of-plane bending" (as described in the Dreiding force field⁴³) is also included. For the sake of simplicity, the geometry of the aromatic systems, as well as the "out of plane bending" of the atoms bonded to the π-carbons of the olefin, has been maintained fixed.

Torsional potentials for the rotation angles are included. For single C_t-C_t bonds not adjacent to a double bond, the following equation was applied

$$E_t = \frac{E'_0}{2}(1 + \cos 3\sigma)$$

while for single bond adjacent to a double bond, the following equation was applied

$$E_t = \frac{E'_0}{2}(1 - \cos 3\sigma)$$

with $E_0 = 2.8$ kcal/mol and $E'_0 = 2.0$ kcal/mol. The torsional potentials for the rotations θ_0 and θ_1 are not known and therefore not included in our calculations. While we expect such energy contribution to be small for θ_1 , it may not be so for θ_0 . Since we are mainly interested in situations not far from 0° (for primary insertion) or not far from 180° (for secondary insertion on the ligand **1**), the inclusion of such a torsional potential would not change significantly our conclusions.

The calculations of the nonbonded energies have been performed with interaction potentials between nonbonded atoms of the Lennard-Jones type. As discussed in ref 44, we have assumed

$$E_{nb} = \sum_{m < n} \left[\left(\frac{A_{ij}}{r_{mn}^{12}} - \frac{B_{ij}}{r_{mn}^6} \right) - \left(\frac{A_{ij}}{r_{ij}^{12}} - \frac{B_{ij}}{r_{ij}^6} \right) \right] \text{ for } r_{mn} < \bar{r}_{ij}$$

$$E_{nb} = 0 \text{ for } r_{mn} \geq \bar{r}_{ij}$$

where A_{ij} and B_{ij} are constants characteristic of the species i

and j and \bar{r}_{ij} the minimum interaction distance. The terms containing \bar{r}_{ij} have been included in order to avoid negative contribution to the energy. The results presented in this paper are obtained with the parameters proposed by Scheraga and co-workers.⁴⁵ In order to test the dependence of the results on the particular choice of the parameters in the potential functions, some calculations have been also performed by using the parameters proposed by Karplus and co-workers,⁴⁶ which have been used in ref 42 together with the bending and stretching parameters for the bridged π-ligands. We also tested the approach proposed by Erker for the coordination of the carbon atoms of the π-ligand,^{47a} in conjunction with the Amber force field of Kollman.^{47b} Although with the different sets of parameters the results are numerically different, the overall trends and the locations of the energy minima are nearly the same. As far as the metal atoms are concerned, it has been shown⁴⁸ for several complexes that the computed conformations of the ligands are practically independent of the nonbonded interactions E_{nb} involving the metal atoms. We have verified this conclusion in our case by some test computations with a range of parameters for the potential functions involving the metal atom (Mt ≡ C, Mt ≡ Cl, Mt as described in refs 42 and 47a, and Mt neglected). Therefore, our final choice has been to completely neglect the interactions involving the metal atom.

The same zero of the energy is adopted in the following for a given model complex, irrespective of the coordination chirality of the propene monomer and of the relative positions of the monomer and growing chain.

The geometrical parameters for the coordination of the ligands **1–4**, taken as starting situations for the energy minimizations, are those found in the crystalline structure of the corresponding dichloro complexes from refs 50, 9, 20, and 20, respectively. The geometric parameters of the coordinated olefin have been derived from the crystal structure of bis-(pentamethyl)cyclopentadienyl(ethene)titanium.⁵¹ The distance C(olefin)-CH₃ has been set to 1.50 Å.

The Zr-C(chain) distance has been assumed, as in ref 21, to be equal to 2.28 Å, which is an average of the values observed in cationic zirconocene complexes.⁵² Since crystalline structures of d⁰ metal-olefin complexes, like those invoked as Ziegler-Natta catalytic intermediates, are not available, it is difficult to assume a reliable distance Zr-C(olefin), which is however expected to be in the range 2.3–2.5 Å, as discussed in detail in ref 21. For the calculations presented in this paper, the distance Zr-C(olefin) has been set to 2.3 Å. Test calculations have been repeated by assuming this distance to be equal to 2.5 Å, obtaining qualitatively similar results.

As in our previous papers,^{7,8,13,15–20,21} possible electronic contributions to the energy have not been considered. This approximation is based on the assumption, which is reasonable according to us, that the differences of electronic energy are negligible in comparing coordination and preinsertion intermediates which are different only for the chiralities of coordination of propene or for the relative positions of the monomer and the growing chain. In principle, however, electronic contributions could lead to minimum energy geometries at the metal atom significantly different from those evaluated by simple molecular mechanics calculations, thus having an indirect influence on the evaluated energy differences. We feel that this is not the case for our models, since the geometry at the metal atom predicted on the sole basis of the nonbonded interactions is very close to that found in similar complexes characterized by X-ray diffraction.⁷

The more complete energy optimizations with respect to previous works^{7,8,15–18} (corresponding to a reduced rigidity of the bridged π-ligand) make smoother the energy curves and markedly reduces the energies for conformations far from the energy minima. However, the differences between the energy minima (corresponding to different diastereoisomeric intermediates) remain substantially unchanged. Nevertheless, we believe that the numerical results of our calculations cannot be trusted as such. This is specially true for conformations far from the energy minima because of the inaptitude of the energy functions in such regions and because of the simplifying assumption of constancy (rather than near-constancy) of several internal coordinates. Although the numerical values

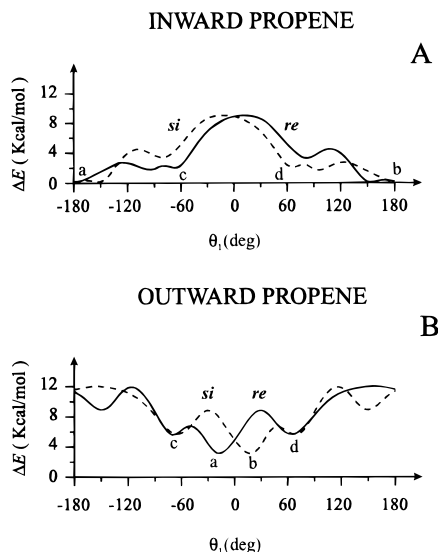


Figure 2. Optimized energy as a function of θ_1 , with $\theta_0 \approx 0^\circ$ (see text), for the model complexes including the *meso*-ethylenebis(η^5 -tetrahydroindenyl) ligand (**1**) with (A) inward propene coordination and (B) outward propene coordination. These models simulate situations suitable for the primary insertion of propene into a polypropylene growing chain. The full and dashed lines refer to *re*- and *si*-coordinated propene, respectively. The conformations corresponding to the energy minima labeled with a–d in A and B are sketched in Figures 3 and 4, respectively.

of the energy differences depend also on the exact geometry and the energy parameters adopted in the calculations, no reasonable adjustment of these parameters seems to be able to modify our conclusions.

Results and Discussion

Model Complexes with the *meso*-Ethylenebis-(4,5,6,7-tetrahydro-1-indenyl) Ligand. For the model complex including the *meso*-ethylenebis(4,5,6,7-tetrahydro-1-indenyl) ligand, for the two diastereoisomeric alkene-bound intermediates corresponding to inward and outward monomer coordinations, plots of the minimized energy versus θ_1 are reported in Figure 2A,B, respectively. The starting point for the energy optimizations in Figure 2 was the conformation with $\theta_0 = 0^\circ$; whatever the energy, the absolute value of θ_0 for the optimized conformations is not greater than 20° . Hence these models simulate situations suitable for the primary insertion of propene into a primary polypropylene growing chain. The full and dashed lines refer to *re*- and *si*-coordinated propene, respectively. For the sake of comparison, let us note that analogous calculations for the alkene-bound intermediate including the corresponding racemic ligand are shown in ref 21.

The minimum energy situation, assumed as zero of the energy in the plots of Figure 2, is found for $\theta_1 \approx 180^\circ$, for the inward (both *re* and *si*) monomer coordination (minima labeled with a and b in Figure 2A, sketched in Figure 3A,B, respectively). For the same alkene-bound intermediate (inward propene), two minima exist also for growing chain conformations which, in the framework of previous analyses of ours, were considered as suitable for the *re*- and *si*-propene insertion, as, for instance, for $\theta_1 = -60^\circ$ and 60° , respectively (minima c and d in Figure 2A, sketched in Figure 3C,D, respectively). These energy minima corresponding to preinsertion intermediates are higher with respect to the absolute minimum of nearly 2 kcal/mol.

For the outward propene coordination, two deep minima (nearly 3 kcal/mol) are present for $\theta_1 \approx -20^\circ$

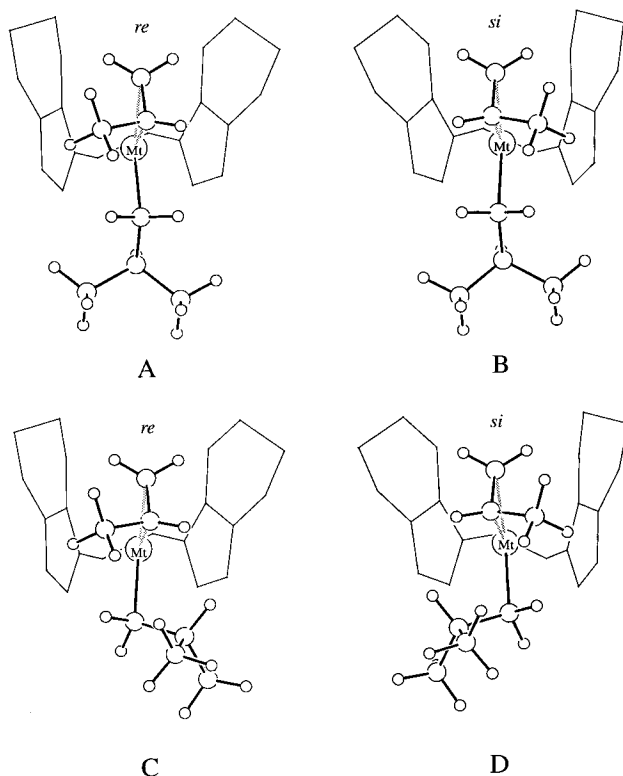


Figure 3. Models corresponding to possible alkene-bound intermediates for the inward monomer coordination when the π -ligand is **1**. A–D correspond to the minimum energy situations labeled with the letters a–d in Figure 2A. C and D are suitable preinsertion intermediates for the *re*- and *si*-monomer insertion, respectively. For clarity, only the C–C bonds are sketched for the π -ligands.

and 20° (shown in Figure 4A,B), for *re*- and *si*-monomer coordinations, respectively. Following the criteria described in the previous section, these alkene-bound intermediates are not considered sufficiently close to the transition state for the insertion reaction. In fact, the second carbon atom of the chain is closer than the first one (although this should become bonded in the insertion reaction) to the coordinated monomer. It is also worth noting that, for the alkene-bound intermediates of Figure 4A,B, the β -hydrogen atom of the chain (indicated with an arrow) points toward the propene monomer (the θ_2 values are nearly equal to 60° and -60° , respectively). This suggests that the minimum energy situations a and b of Figure 2B, sketched in Figure 4A,B, could be close to a possible transition state for a termination reaction, through a β -H abstraction, rather than to a possible transition state for the monomer insertion.

Suitable preinsertion intermediates corresponding to the *re*- and *si*-propene outward coordinations, with $\theta_1 \approx -60^\circ$ or 60° , respectively (minima labeled with c and d in Figure 2B, sketched in Figure 4C,D, respectively) present energies of nearly 5–6 kcal/mol higher than the absolute minimum. In this case, the β -hydrogen atom of the chain (indicated with an arrow) points toward a tetrahydroindenyl ligand (the θ_2 values are nearly equal to -30° and 30° , respectively).

Although it is well established that, in general, the activation internal energy for the monomer coordination to the metallocene-based catalytic sites is expected to be low,^{26,27,53} the activation free energy (especially at low monomer concentrations) may be such as to render the back-skip process significant. Moreover, the larger nonbonded energy contribution to the preinsertion intermediate with the outward monomer coordination

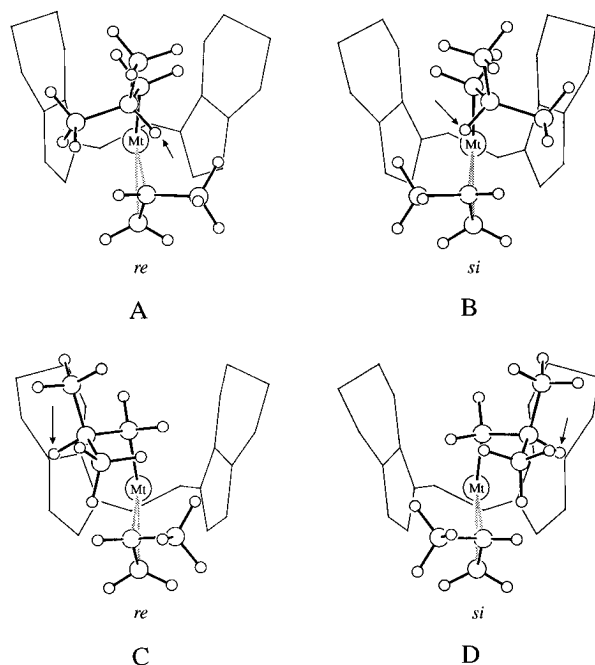


Figure 4. Models corresponding to possible alkene-bound intermediates for the outward monomer coordination when the π -ligand is **1**. A–D correspond to the minimum energy situations labeled with the letters a–d in Figure 2B. A and B are alkene-bound intermediates possibly close to the transition state of the β -H elimination reaction, while C and D are models of preinsertion intermediates for the *re*- and *si*-monomer insertion, respectively. For clarity, only the C–C bonds are sketched for the π -ligands.

($E_{\text{out}} > E_{\text{inw}}$) suggests that, in the alkene-free state, the activation energy for its formation, $E_a(\text{coord.,out})$, could get comparable with the activation energy for the back-skip of the chain, $E_a(\text{bs})$ (see Scheme 2).

Figure 5A,B contains plots of the optimized energies for the intermediates with the inward and outward propene coordinations, respectively, as a function of θ_0 . For the inward propene coordination, deep energy minima are obtained only for $\theta_0 \approx 0^\circ$, while much higher energies are calculated for $\theta_0 \approx 180^\circ$. This, of course, is due to the interactions of the methyl group of the propene (for both *re* and *si* coordinations) with the atoms of one of the two six-membered rings for the monomer orientation suitable for the secondary insertion ($\theta_0 \approx 180^\circ$). On the contrary, for the outward propene coordination, the energy minima in the neighborhood of $\theta_0 = 180^\circ$ (for $\theta_0 \approx 170^\circ$ and -170°) are only 2–3 kcal/mol higher than those in the neighborhood of $\theta_0 = 0^\circ$ (for $\theta_0 \approx 10^\circ$ and -10°). It is hence apparent that there are strong nonbonded energy contributions to the regioselectivity for the inward monomer coordination (Figure 5A, compare $\theta_0 \approx 0^\circ$ with $\theta_0 \approx 180^\circ$), while much smaller nonbonded energy contributions to the regioselectivity have been calculated for the outward monomer coordination (Figure 5B). The latter is similar to the nonbonded energy contribution to the regioselectivity calculated for the model with the corresponding racemic ligand (Figure 3A in ref 21).

Hence, the studied *meso*-ligand model appears to be nonenantioselective, but if the frequency of the back-skip of the chain increases, its regioselectivity becomes larger than the regioselectivity of the racemic ligand model. This is in qualitative agreement with the microstructure of the polymer obtained by the corresponding catalytic systems. In fact, the atactic polymer produced with *meso*-ethylenebis(4,5,6,7-tetrahydro-1-

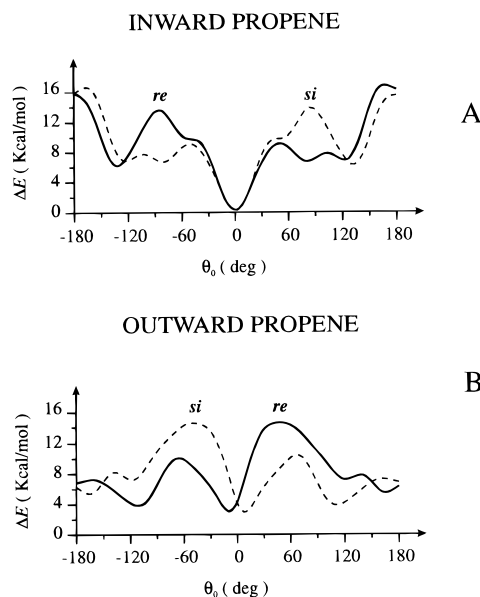


Figure 5. Optimized energy as a function of θ_0 for the model complexes with the ligand **1** with (A) inward propene coordination and (B) outward propene coordination. The full and dashed lines refer to *re*- and *si*-coordinated propene, respectively.

indenyl)zirconium dichloride is more regioregular than the polymer obtained with its racemic isomer.⁵⁰

Although our calculations have been performed separately for the δ and λ conformations of the ethylene bridge, since the isomerization between the two conformers is assumed to be easy, only the minimum energy values are reported in the curves of Figures 2 and 5. For the sake of comparison with the results of following sections, it is however worth noting that substantially no enantioselectivity is introduced by freezing in the model the ethylene bridge conformation of the π -ligand.

Model Complex with the Isopropylidene[(3-methyl(η^5 -cyclopentadienyl))(η^5 -9-fluorenyl)] Ligand. As described in the section relative to the methods, without loss of generality, all the calculations, reported in this section and the next two sections, refer to the *R* coordination of the ligand.

For the model complex with the isopropylidene[(3-methyl(η^5 -cyclopentadienyl))(η^5 -9-fluorenyl)] ligand, for the two diastereoisomeric intermediates corresponding to inward and outward monomer coordinations, plots of the minimized energy versus θ_1 (analogous to those of Figure 2A,B) are reported in Figure 6A,B, respectively. In agreement with previous less-refined calculations,¹³ it is apparent that for the inward monomer coordination this model site is enantioselective. In particular, the calculated energy difference between the two preinsertion intermediates suitable for the *re*- and *si*-monomer insertion (*re* olefin, $\theta_1 \approx -60^\circ$, labeled as a in Figure 6A and sketched in Figure 7A, and *si* olefin, $\theta_1 \approx +60^\circ$ is nearly 7 kcal/mol. On the other hand, this model site, for the outward coordination of the monomer, is substantially nonenantioselective, that is, two nearly energetically equivalent preinsertion intermediates corresponding to the situations (*re* olefin, $\theta_1 \approx -60^\circ$, and *si* olefin, $\theta_1 \approx 60^\circ$, labeled as b and c in Figure 6B and sketched in Figure 7B,C, respectively) are present. The energies for the two minima of the nonenantioselective step (Figure 6B), with respect to the single minimum of the enantioselective step (Figure 6A), are higher by nearly 4 kcal/mol.

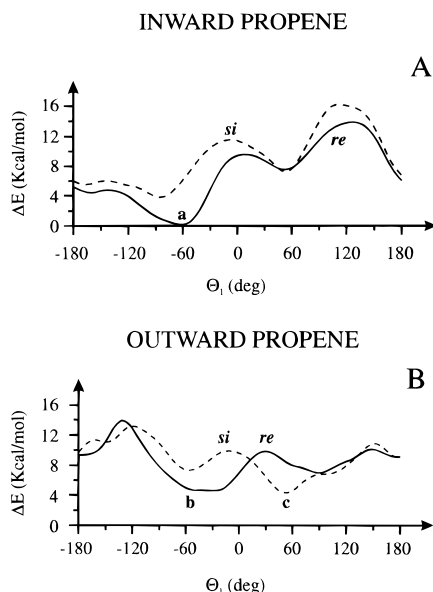


Figure 6. Optimized energy as a function of θ_1 , with $\theta_0 \approx 0^\circ$ (see text), for the model complexes with the isopropylidene-[(3-methyl(η^5 -cyclopentadienyl))(η^5 -9-fluorenyl)] ligand (2), *R* coordinated, for the (A) inward propene coordination and (B) outward propene coordination. The full and dashed lines refer to *re*- and *si*-coordinated propene, respectively. The conformations corresponding to the energy minimum situations labeled with a–c are sketched in Figure 7.

These results are in qualitative agreement with the appreciable probability of two successive enantioselective additions and the near to zero probability of two successive nonenantioselective additions, calculated from experimental observations for the corresponding catalytic system.^{9,14} This system, although essentially hemi-isospecific (hence, in the framework of our analysis, roughly rationalized by a model of the kind iii), presents a large amount of skipped insertions.^{9,14} In particular, according to the accurate analysis by Farina and co-workers¹⁴ on experimental data by Ewen⁹ (relative to a system with catalyst + MAO, without solvent, at 65 °C), the probability of two successive enantioselective additions is close to 15%, while the probability of two successive nonenantioselective additions is essentially zero.

Model Complexes with the Ethylene[1-(η^3 -9-fluorenyl)-1-phenyl-2-(η^5 -1-indenyl)] Ligand. The model catalytic complexes considered in this section correspond to the diastereoisomeric complexes 6b1 and 6b2 of ref 20 and present a *R* chirality of coordination of the indenyl fragment. The model sites based on the ethylene[1-(η^5 -9-fluorenyl)-1(*R*)-phenyl-2-(η^5 -1(*R*)-indenyl)] ligand presenting a δ -bridge conformation and the model sites based on the ethylene[1-(η^5 -9-fluorenyl)-1(*S*)-phenyl-2-(η^5 -1(*R*)-indenyl)] ligand presenting a λ -bridge conformation are sketched in Figures 8 and 9 and hereafter named **3 δ** and **3 λ** , respectively. For the model site **3 δ** , plots of the optimized energy versus θ_1 (analogous to those of Figure 2A,B) are reported in Figure 8A,B for the two diastereoisomeric intermediates corresponding to inward and outward monomer coordinations, respectively. For the model site **3 λ** , analogous plots of the optimized energy versus θ_1 for the inward and outward monomer coordinations are reported in Figure 9A,B, respectively.

In the framework of our analysis, the diastereoisomeric intermediates corresponding to the inward monomer coordination (Figures 8A and 9A) are enantioselective. In fact, the preinsertion intermediate for the *re*-monomer insertion, with $\theta_1 \approx -60^\circ$ (a in Figures 8A

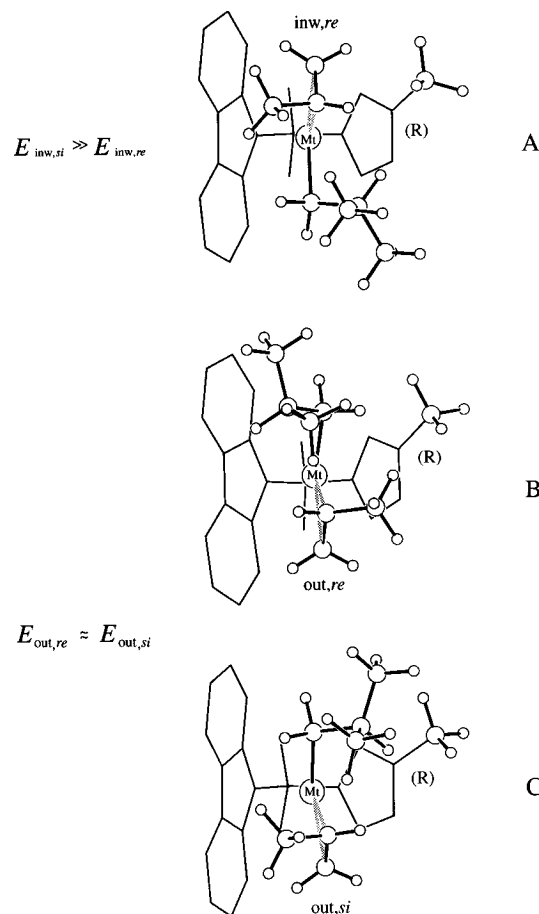


Figure 7. Models of preinsertion intermediates for the primary insertion of propene into a polypropylene growing chain when the π ligand is 2. A–C correspond to the minimum energy situations labeled with the letters a–c in Figure 6. The model A corresponds to the inward coordination of the *re* monomer, while the two nearly energetically equivalents models B and C correspond to the outward coordination of the *re* and *si* monomers, respectively. For clarity, only the C–C bonds are sketched for the π -ligands.

and 9A, sketched in Figures 10A and 11A, respectively), presents energies lower by 4.5–6.5 kcal/mol with respect to the preinsertion intermediate for the *si*-olefin insertions, with $\theta_1 \approx 60^\circ$.

On the contrary, the diastereoisomeric intermediates corresponding to the outward monomer coordinations (Figures 8B and 9B) might have opposite, although poor, enantioselectivities. In particular, for the δ -bridge conformation, the preinsertion intermediate for the *re*-monomer insertion, with $\theta_1 \approx -60^\circ$ (b in Figure 8B, sketched in Figure 10B), presents an energy lower by nearly 1.5 kcal/mol with respect to the preinsertion intermediate for the *si*-olefin insertions, with $\theta_1 \approx 60^\circ$ (c in Figure 8B, sketched in Figure 10C). On the other hand, for the λ -bridge conformation, the preinsertion intermediate for the *si*-monomer insertion (c in Figure 9B, sketched in Figure 11C) presents an energy lower by nearly 1 kcal/mol with respect to the preinsertion intermediate for the *re*-olefin insertions (b in Figure 9B, sketched in Figure 11B).

Hence a substantial influence of the bridge conformation on the enantioselectivity of the model complex appears to occur only when the growing chain is located in the more crowded inward position (and, of course, the monomer is coordinated in the outward position). In particular, for the *R*-ligand coordination, the δ -bridge conformation tends to favor the chain conformation with $\theta_1 \approx -60^\circ$ (Figure 10B) with respect to the one with θ_1

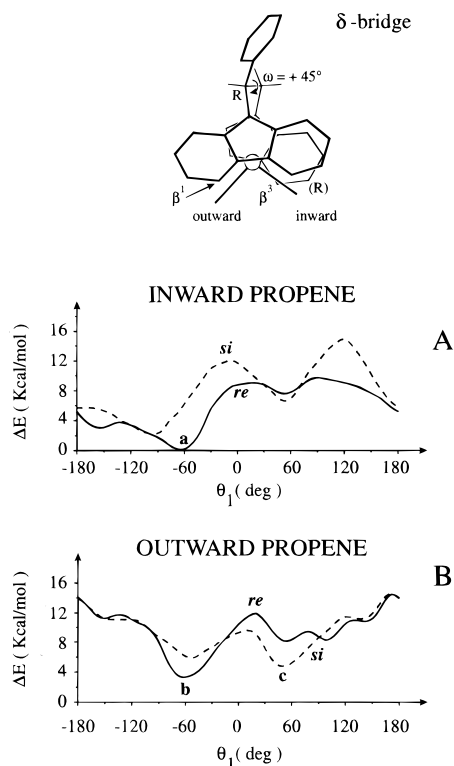


Figure 8. Optimized energy as a function of θ_1 , with $\theta_0 \approx 0^\circ$ (see text), for the model complexes including the ethylene[1-(η^5 -9-fluorenyl)-1(*R*)-phenyl-2-(η^5 -1-indenyl)] ligand (**3**) (*R* coordinated), with δ -bridge conformation, for the (A) inward propene coordination and (B) outward propene coordination. The full and dashed lines refer to *re*- and *si*-coordinated propene, respectively. The sketch of the model site indicates the ω value, the inward and outward coordination positions, the chirality of coordination of the indenyl fragment (*R*), the chirality of the tertiary carbon atom of the bridge (*R*), and the position of the opposite standing Cp substituents β^1 and β^3 . The preinsertion intermediates corresponding to the energy minima labeled with a–c are sketched in Figure 10.

$\approx 60^\circ$ (Figure 10C), due to the lower interactions of the second carbon atom of the chain (and of its substituents) with the six-membered rings of the π -ligand. The opposite occurs for the ligand with the λ -bridge conformation, which tends to favor the chain conformation with $\theta_1 \approx 60^\circ$ (Figure 11C) with respect to the one with $\theta_1 \approx -60^\circ$ (Figure 11B). This orientation of the growing chain, in turn, discriminates between *re*- and *si*-monomer insertions; in particular the *re*-monomer insertion is favored for the site **3 δ** , while the *si*-monomer insertion is favored for the site **3 λ** .

Calculations analogous to those of Figures 8 and 9 when the growing chain is simulated only by a methyl group indicate a substantial absence of enantioselectivity (that is, nearly equivalent preinsertion intermediates for the *re*- and *si*-monomer insertion) for both inward and outward coordination of the monomer, for both δ and λ sites. Hence, according to the present analysis, the influence of the bridge conformation (as well as of the chirality of coordination of the bridged π -ligand^{7,21}) on the enantioselectivity seems to be mainly mediated by the chiral orientation of the growing chain.

In summary the model sites **3 δ** and **3 λ** would be both essentially hemi-isospecific (in fact, as for the ligand **2**, the monomer insertion with a given enantioface is largely favored for the inward coordination, while for the outward monomer coordination the two energy minima suitable for the insertion reaction are energetically nearly equivalent). However for the model **3 δ** some tendency to the isospecificity is found (in fact, for

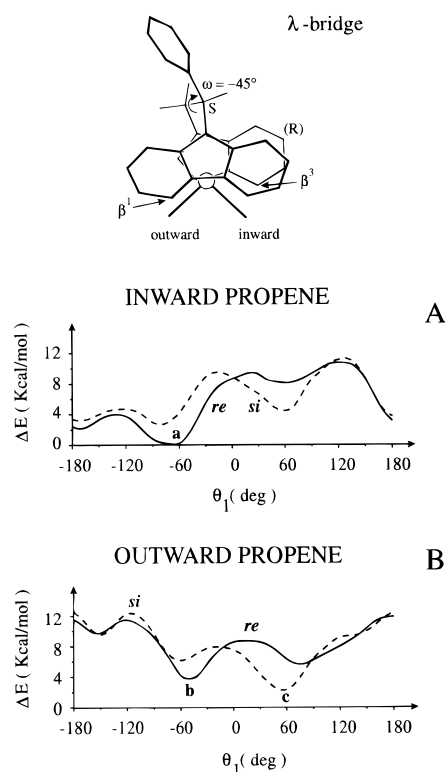


Figure 9. Optimized energy as a function of θ_1 , with $\theta_0 \approx 0^\circ$ (see text), for the model complexes including the ethylene[1-(η^5 -9-fluorenyl)-1(*S*)-phenyl-2-(η^5 -1-indenyl)] ligand (*R* coordinated), with λ -bridge conformation, for the (A) inward propene coordination and (B) outward propene coordination. The full and dashed lines refer to *re*- and *si*-coordinated propene, respectively. The sketch of the model indicates the ω value, the inward and outward coordination positions, the chirality of coordination of the indenyl fragment (*S*), the chirality of the tertiary carbon atom of the bridge (*S*), and the position of the opposite standing substituents β^1 and β^3 . The preinsertion intermediates corresponding to the energy minima labeled with a–c are sketched in Figure 11.

instance, for the *R*-ligand coordination, the *re*-monomer insertion is largely favored for the inward coordination and less, but still, favored for the outward coordination).

These results are in good qualitative agreement with the stereospecificities of the corresponding catalytic systems (at 50°C , with methylalumoxane, for monomer concentrations higher than 2–3 M): The percentage of [mmmm] pentads is 46.5% and 15.5% for the δ - and λ -bridge conformations, respectively.²⁰ It is worth noting that [mmmm] $\approx 15\%$ is typical of hemi-isospecific polymers.^{9,14}

It is also worth recalling that the overall higher enantioselectivity of the model complex **3 δ** , with respect to the model complex **3 λ** , can be more qualitatively accounted for by the simple considerations of Brintzinger:³⁰ the δ conformation, with respect to the λ one, places closer the opposite standing substituents β^1 and β^3 (sketches in Figures 8 and 9), thus placing both the monomer and the growing chain in a more crowded environment.

Other relevant information, which can be taken from Figures 8 and 9, is the energy difference (for the catalytic model complexes **3 δ** and **3 λ** , respectively) between the energy minima for the inward and outward monomer coordinations. It is apparent from Figures 8 and 9 that the absolute minima, labeled as a, correspond to the inward monomer coordination for both bridge conformations. The preinsertion intermediates for the outward monomer coordination have energies higher by nearly 3 and 2 kcal/mol (minimum b of Figure 8B and

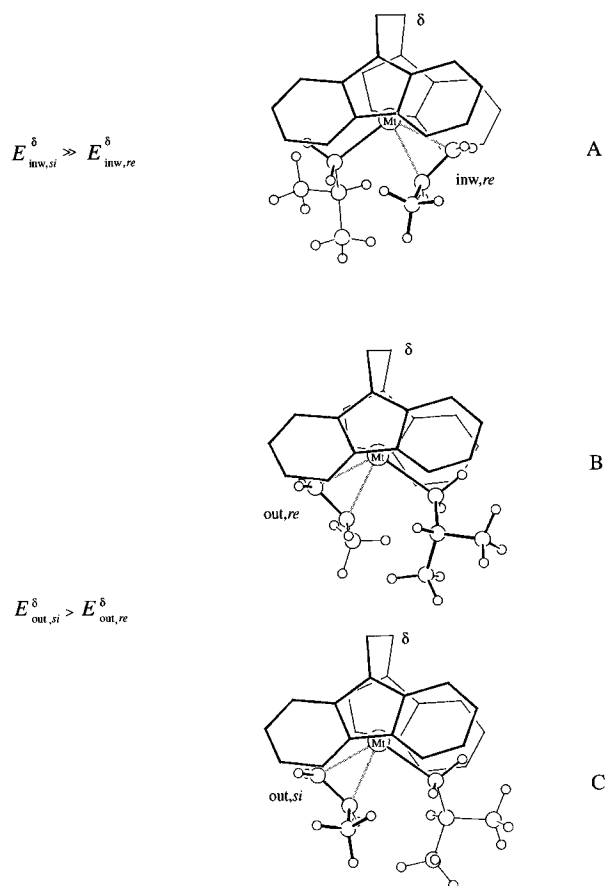


Figure 10. Models of the preinsertion intermediates for the primary insertion of propene into a polypropylene growing chain when the π ligand is **3** with a δ -bridge conformation. A–C correspond to the minimum energy situations labeled with the letters a–c in Figure 8. The model A corresponds to the inward coordination of the *re* monomer, while the models B and C correspond to the outward coordination of the *re* and *si* monomers, respectively. For clarity, only the C–C bonds are sketched for the π -ligands. Thinner lines indicate bonds connecting atoms which in the sketches are below the metal atom.

minimum c of Figure 9B), for δ - and λ -bridge conformations, respectively. In our framework, this indicates that a phenomenon of back-skip of the chain could occur toward the enantioselective diastereoisomeric intermediate, presenting the inward monomer coordination.

This is, again, in good qualitative agreement with the increasing isospecificities of the corresponding catalytic systems with decreasing the monomer concentration. In fact, by reducing the monomer concentration (from 3.38 to 0.45 M), there is an increase of the percentage of [mmmm] pentads for both catalytic systems (from 46.5% up to 80.4% with the ligand **3** δ and from 15.5% up to 28.3% with the ligand **3** λ).²⁰

Already in Scheme 3 of ref 20, the increase of the stereospecificity of these catalytic systems with the decrease of the monomer concentration was rationalized in terms of increase of the frequency of occurrence of a back-skip of the chain (in the alkene-free state) from the coordination position typical of the higher energy diastereoisomeric intermediate (nonenantioselective) toward the coordination position typical of the minimum energy diastereoisomeric intermediate (enantioselective). However, in that reaction scheme, the minimum energy enantioselective intermediate was supposed to be that one with the outward monomer coordination, which, on the contrary, according to our analysis, would be of higher energy and nonenantioselective.

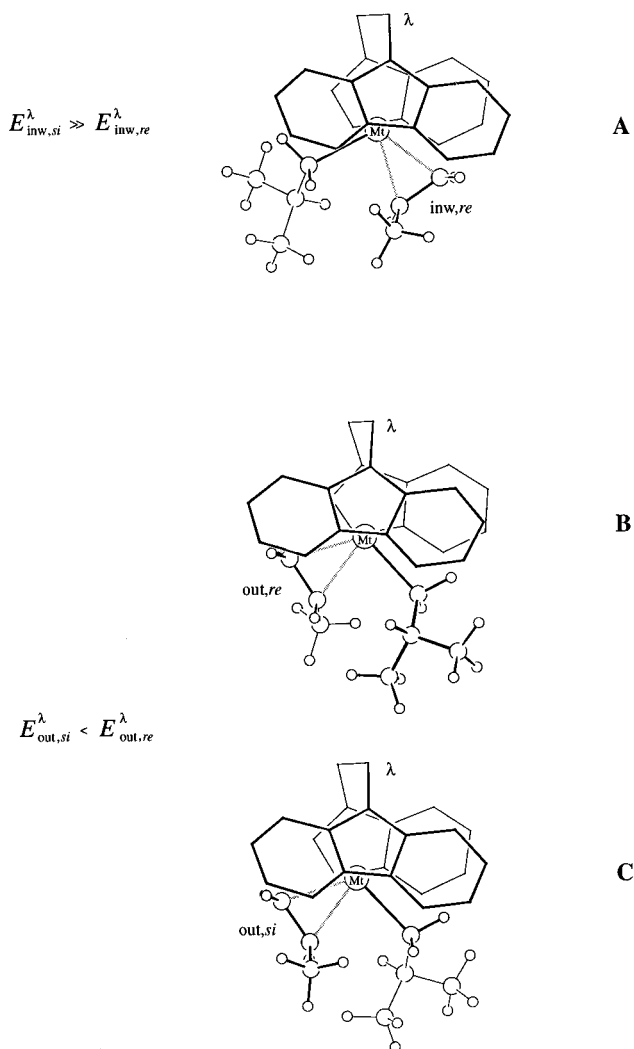


Figure 11. Models of the preinsertion intermediates for the primary insertion of propene into a polypropylene growing chain when the π ligand is **3** with a λ -bridge conformation. A–C correspond to the minimum energy situations labeled with the letters a–c in Figure 9. The model A corresponds to the inward coordination of the *re* monomer, while the models B and C correspond to the outward coordination of the *re* and *si* monomers, respectively. For clarity, only the C–C bonds are sketched for the π -ligands. Thinner lines indicate bonds connecting atoms which in the sketches are below the metal atom.

Before concluding this section, let us recall that the complex with a *S* coordination of the indenyl fragment having a δ (λ)-bridge conformation is the enantiomer of the complex with *R* chirality of coordination of the indenyl fragment having a λ (δ) conformation. As a consequence, for the case of the ligand *S* coordinated, the model site with the λ -bridge conformation is more isospecific (in favor of the *si*-monomer insertion).

Model Complex with the Ethylene[1-(η^5 -cyclopentadienyl)-1-phenyl-2-(η^5 -1-indenyl)] Ligand. For the model complex based on the ethylene[1-(η^5 -cyclopentadienyl)-1-phenyl-2-(η^5 -1-indenyl)] ligand (*R* coordinated), with δ -bridge conformation, for the two diastereoisomeric intermediates corresponding to inward and outward monomer coordinations, plots of the minimized energy versus θ_1 are reported in Figure 12A,B, respectively. For the same model complex with λ -bridge conformation, analogous plots of the minimized energy versus θ_1 for the inward and outward monomer coordinations are reported in Figure 13A,B, respectively.

In the framework of our analysis, one of the diastereoisomeric intermediates (that one corresponding to the

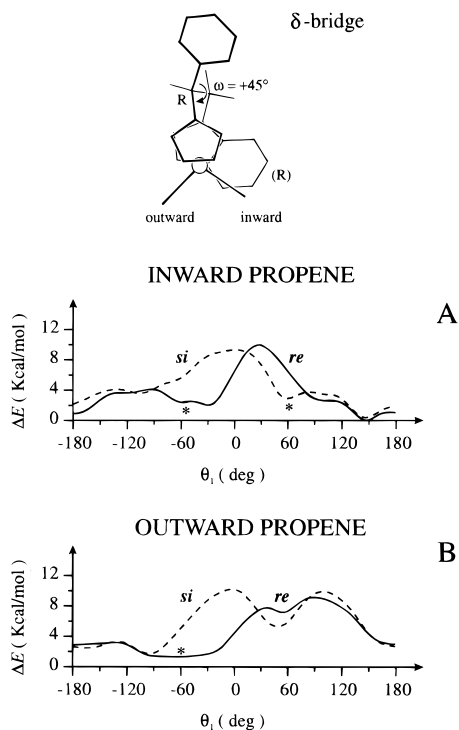


Figure 12. Optimized energy as a function of θ_1 , with $\theta_0 \approx 0^\circ$ (see text), for the model complexes including the ethylene-[1-(η^5 -cyclopentadienyl)-1-phenyl-2-(η^5 -1-indenyl)] ligand (R coordinated), with δ -bridge conformation, for the (A) inward propene coordination and (B) outward propene coordination. The full and dashed lines refer to *re*- and *si*-coordinated propene, respectively. The asterisks indicate suitable preinsertion intermediates. The sketch of the model indicates the ω value, the inward and outward coordination positions, the chirality of coordination of the indenyl fragment (R), and the chirality of the tertiary carbon atom of the bridge (R).

outward monomer coordination) is enantioselective (Figures 12B and 13B). In fact, the preinsertion intermediates for the *re*-monomer insertion (with $\theta_1 \approx -60^\circ$) present lower energies with respect to the preinsertion intermediates for the *si*-olefin insertions (with $\theta_1 \approx 60^\circ$). This energy difference related to the enantioselectivity is higher for the δ -bridge conformation (≈ 4 kcal/mol) and lower for the λ -bridge conformation (≈ 2 kcal/mol).

On the contrary, the diastereoisomeric intermediates corresponding to the inward monomer coordinations (Figures 12A and 13A) present essentially no enantioselectivity for both bridge conformations. This is due to the absence, for the chain in the outward position, of steric interactions which could induce its possible chiral orientation.

Hence, in the framework of our analysis, the model sites with the ligand **4**, both with δ - and λ -bridge conformation, are essentially hemi-isospecific. The model site with the δ -bridge conformation presents, however, a slightly higher tendency to the obtaining of *m* rich pentads. These results are only in qualitative agreement with the stereospecificities of the corresponding catalytic systems (at 50°C , with methylalumoxane, for monomer concentrations higher than 2–3 M): The percentage of [mmmm] pentads is, in fact, close to 40% and 35% for the δ - and λ -bridge conformations, respectively.²⁰

Other relevant information, which can be taken from Figures 12 and 13, is the small energy difference (for the catalytic complexes **4 δ** and **4 λ** , respectively) between the energy minima for the preinsertion intermediates corresponding to the inward and outward monomer coordinations (indicated by asterisks). Moreover, con-

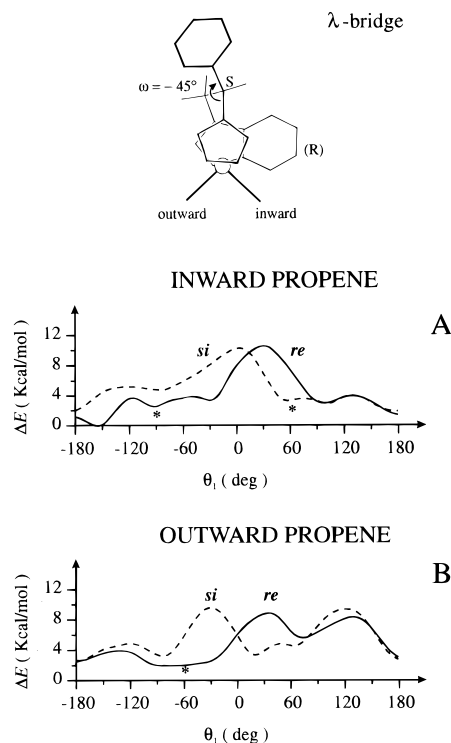


Figure 13. Optimized energy as a function of θ_1 , with $\theta_0 \approx 0^\circ$ (see text), for the model complexes including the ethylene-[1-(η^5 -cyclopentadienyl)-1-phenyl-2-(η^5 -1-indenyl)] ligand (R coordinated), with λ -bridge conformation, for the (A) inward propene coordination and (B) outward propene coordination. The full and dashed lines refer to *re*- and *si*-coordinated propene, respectively. The asterisks indicate suitable preinsertion intermediates. The sketch of the model site indicates the ω value, the inward and outward coordination positions, the chirality of coordination of the indenyl fragment (R), and the chirality of the tertiary carbon atom of the bridge (S).

trary to the cases of ligands **2** and **3**, this small difference is in favor of the nonenantioselective step. In our framework, this indicates a poor nonbonded energy contribution to the activation energy for the monomer coordination, which remains low with respect to the activation energy for the back-skip of the chain. Hence, also for small monomer concentrations, the rate of the monomer coordination (and insertion) is expected to be higher than the rate of the chain back-skip. These results are in qualitative agreement with the invariance of the stereospecificities of the corresponding catalytic systems with decreasing the monomer concentration, for the catalytic system with the ligand **4**.

Conclusions

The main results of the present molecular mechanics analysis on model metallocene intermediates for the propene polymerization, in which the two coordination positions available for the monomer and the growing chain are diastereotopic, are summarized in Table 1.

In particular, the calculated energy differences between suitable preinsertion intermediates for the primary *si*- and *re*-monomer insertions, for inward and outward monomer coordinations (for the case of R coordination of the ligands), are collected in the second and third columns. These energy differences represent an evaluation of the enantioselectivity of the diastereoisomeric intermediates corresponding to two consecutive insertion steps, in the framework of the chain migratory insertion mechanism. The experimentally observed stereospecificities (expressed as percent of [mmmm] pentads) for corresponding catalytic systems

Table 1. Calculated Energy Differences (in kcal/mol) between Preinsertion Intermediates for the Considered Model Complexes (for the *R* coordination of the ligands) Related to the Enantioselectivities (and stereospecificity) and the Possible Occurrence of the Back-Skip of the Chain of the Corresponding Catalytic Systems

model complex	enantioselectivity		experimental [mmmm]%	occurrence of back-skip	
	$E_{\text{inw},si} - E_{\text{inw},re}$	$E_{\text{out},si} - E_{\text{out},re}$		$E_{\text{out}} - E_{\text{inw}}$	experimental observations
1	0	0	aspecific	4.0	
2	7.2	-0.3	14 ^a	4.3 ^c	<i>e</i>
3δ	6.5	1.5	46.5 ^b	3.1 ^c	<i>f</i>
3λ	4.4	-1.0	15.5 ^b	2.2 ^c	<i>g</i>
4δ	0.5	3.8	39.3 ^b	0.7 ^d	<i>h</i>
4λ	-0.1	2.0	34.4 ^b	0.5 ^d	<i>h</i>

^a Substantially hemi-isospecific. Polymerization at 65 °C without solvent.⁹ ^b Polymerization at 50 °C with methylalumoxane and monomer concentration = 3.38 M.²⁰ ^c The more enantioselective insertion step is energetically favored. ^d The less enantioselective insertion step is energetically favored. ^e Appreciable probability ($\approx 15\%$) of two successive enantioselective additions and essentially null probability of two successive nonenantioselective additions. Increase of [mmmm]% with reducing monomer concentration is predicted. ^f [mmmm]% from 46.5 up to 80.4 for monomer concentration reducing from 3.38 to 0.45 M.²⁰ ^g [mmmm]% from 15.5 up to 28.3 for monomer concentration reducing from 3.38 to 0.45 M.²⁰ ^h [mmmm]% nearly constant with monomer concentration.²⁰

are listed in the fourth column. It is apparent that the calculated enantioselectivities are in fair agreement with the observed aspecificity of the catalytic systems based on **1** and with the hemi-isospecificity of the catalytic systems based on **2**.

The molecular mechanics analysis shows that the nonbonded interactions are also able to account for the influence of the ethylene bridge conformation on the stereospecificity of the propene polymerization in *ansa*-zirconocene complexes. According to the calculations, a significant influence of the bridge conformation on the enantioselectivity of the preinsertion intermediates is present only in crowded catalytic model complexes. In fact, such influence is poor for the model complexes based on **1** and **4**, while it is relevant for the crowded model complex based on **3**, particularly for the model presenting the growing chain in the more crowded inward position (outward propene coordination). In particular, the complex including the ligand **3**, with δ -bridge conformation, for the outward monomer coordination is partially enantioselective (1.5 kcal/mol) in favor of the same enantioface (*re*) strongly favored for the inward monomer coordination, while with λ -bridge conformation, the model complex with the outward monomer coordination is partially enantioselective (1 kcal/mol) in favor of the opposite enantioface (*si*) (Table 1). Hence the model **3 λ** is essentially hemi-isospecific, while the model **3 δ** tends to be more isospecific. Analogously, for model **4 δ** with respect to model **4 λ** , a slightly larger tendency to the isospecificity has been calculated. All these results are in qualitative agreement with the stereospecificities of the corresponding catalytic systems (fourth column of Table 1). It is worth noting that, according to the present analysis, the influence of the bridge conformation on the enantioselectivity seems to be mainly mediated by the chiral orientation of the growing chain (as nearly generally accepted for the influence of the chirality of the site on the enantioselectivity).

For the same model complexes, the calculated energy differences between suitable preinsertion intermediates for the primary monomer insertion for inward and

outward monomer coordinations are collected in the fifth column of Table 1. These results indicate that, in all the considered metallocene-based model complexes, when there are energy differences between the minimum energy diastereoisomeric intermediates, lower energies correspond to the monomer coordination in the inward coordination position. The energy difference between the two possible diastereoisomeric preinsertion intermediates is somewhat relevant for the model complexes based on the *meso*-ethylenebis(4,5,6,7-tetrahydro-1-indenyl) ligand (**1**), the isopropylidene[(3-methyl(η^5 -cyclopentadienyl))(η^5 -9-fluorenyl)] ligand (**2**), or the *rac*-ethylene[1-(η^5 -9-fluorenyl)-1-phenyl-2-(η^5 -1-indenyl)] ligand (**3**), and for models **2** and **3** the energy difference is in favor of the more enantioselective step. On the contrary, this energy difference is small and in favor of the substantially nonenantioselective step for the model complexes based on the *rac*-ethylene[1-(η^5 -cyclopentadienyl)-1-phenyl-2-(η^5 -1-indenyl)] ligand (**4**).

Large energy differences between the minima of the diastereoisomeric coordination (and preinsertion) intermediates (ΔE) could correspond to substantial nonbonded energy contributions to the activation energy for the formation of the higher energy alkene-bound intermediate ($E_a(\text{coord.,out})$). As a consequence, the rate of monomer coordination can become comparable (or also lower) with respect to the rate of the back-skip of the chain toward the less hindered coordination position in the alkene-free state.

Several experimental facts relative to the propene polymerization behavior of the corresponding catalytic systems (sixth column in Table 1) can be rationalized by considering the kinetic competition between the back-skip of the chain and the monomer coordination in the alkene-free state. In particular, the appreciable probability of two successive additions at the enantioselective catalytic face and the near to zero probability of two successive additions at the nonenantioselective catalytic face, observed for the essentially hemi-isospecific catalytic system based on **2**, are rationalized in terms of the lower energies for the single minimum of the enantioselective steps with respect to the two minima of the nonenantioselective steps. The increased stereoregularity at decreasing monomer concentration for catalytic systems based on **3** (not shown by systems based on **4**) can be explained on similar grounds. The higher regioregularity of the polypropylene obtained by the zirconocene catalyst based on **1** (compared to the polymer obtained with the catalytic system containing its racemic isomer) could be also rationalized in terms of a strong nonbonded energy contribution to the regioregularity for the lower energy alkene-bound intermediate, corresponding to the inward coordination of the monomer.

A polymerization mechanism with a frequent back-skip of the chain could operate in other isospecific catalytic systems with non- C_2 -symmetric metallocenes like those of refs 54–60. However, for these systems the isospecificity could be otherwise related to the presence of different enantioselectivities for the two diastereoisomeric situations but in favor of a same prochiral face. Hence, for a possible discrimination between the two alternative mechanisms for the isospecificity, specific molecular mechanics analyses would be needed for each catalytic model site.

The possible occurrence, for peculiar metallocene complexes, of a polymerization mechanism with a back-skip of the chain has relevant implications on the selection of suitable isospecific model sites between those proposed several years ago for the heterogeneous

Ziegler–Natta catalysis. In fact, beside model sites with two homotopic coordination positions (available for the monomer and the growing chain),⁶ one can consider, as suitable for the isospecific heterogeneous Ziegler–Natta catalysis, also model sites with two diastereotopic coordination positions,^{1,2,15–18} which are isospecific only by assuming a polymerization mechanism with a regular back-skip of the chain.

Let us also suggest that a change from a polymerization mechanism with a chain migratory insertion toward one with a regular back-skip of the chain could be also responsible for the change of stereospecificity, from syndio to iso, which occurs when syndiospecific metallocene catalysts (with bridged cyclopentadienylfluorenyl ligands) are supported on SiO₂.⁶¹

Acknowledgment. We thank Dr. J. A. Ewen of the Catalyst Research Corp. and Dr. L. Resconi of Montell Polyolefins, G. Natta Research Center, for useful discussions. The financial supports of the Progetto Strategico Tecnologie Chimiche Innovative, and the Ministero dell'Università e della Ricerca Scientifica e Tecnologica of Italy and of Montecatini Spherilene are also acknowledged.

References and Notes

- (1) Cossee, P. *J. Catal.* **1964**, *3*, 80.
- (2) Cossee, P. In *The Stereochemistry of Macromolecules*; Ketley, A. D., Ed.; Marcel Dekker: New York, 1967; Vol. 1, Chapter 3.
- (3) Natta, G.; Farina, M.; Peraldo, M. *Chim. Ind. (Milan)* **1960**, *42*, 255.
- (4) Zambelli, A.; Giongo, M. G.; Natta, G. *Makromol. Chem.* **1968**, *112*, 183.
- (5) Mislow, K.; Raban, M. *Top. Stereochem.* **1967**, *1*, 1.
- (6) Allegra, G. *Makromol. Chem.* **1971**, *145*, 235.
- (7) Corradini, P.; Guerra, G.; Vacatello, M.; Villani, V. *Gazz. Chim. Ital.* **1988**, *118*, 173.
- (8) Cavallo, L.; Corradini, P.; Guerra, G.; Vacatello, M. *Polymer* **1991**, *32*, 1329.
- (9) Ewen, J. A.; Elder, M. J.; Jones, R. L.; Haspeslagh, L.; Atwood, J. L.; Bott, S. G.; Robinson, K. *Makromol. Chem., Macromol. Symp.* **1991**, *48/49*, 253.
- (10) Ewen, J. A. *J. Am. Chem. Soc.* **1984**, *106*, 6355.
- (11) Kaminsky, W.; Kulper, K.; Brintzinger, H. H.; Wild, F. R. W. P. *Angew. Chem., Int. Ed. Engl.* **1985**, *24*, 507.
- (12) Ewen, J. A.; Jones, R. L.; Razavi, A.; Ferrara, J. D. *J. Am. Chem. Soc.* **1988**, *110*, 6255.
- (13) Cavallo, L.; Corradini, P.; Guerra, G.; Vacatello, M. *Macromolecules* **1991**, *24*, 1784.
- (14) Farina, M.; Di Silvestro, G.; Sozzani, P. *Macromolecules* **1993**, *26*, 946.
- (15) Corradini, P.; Barone, V.; Fusco, R.; Guerra, G. *Eur. Polym. J.* **1979**, *15*, 133.
- (16) Corradini, P.; Barone, V.; Fusco, R.; Guerra, G. *J. Catal.* **1982**, *77*, 32.
- (17) Corradini, P.; Guerra, G.; Villani, V. *Macromolecules* **1985**, *18*, 1401.
- (18) Corradini, P.; Barone, V.; Fusco, R.; Guerra, G. *Gazz. Chim. Ital.* **1983**, *113*, 601.
- (19) Corradini, P.; Guerra, G.; Cavallo, L.; Moscardi, G.; Vacatello, M. In *Ziegler Catalysts*; Fink, G., Mülhaupt, R., Brintzinger, H. H., Eds.; Springer-Verlag: Berlin, 1995; p 237.
- (20) Rieger, B.; Jany, G.; Fawzi, R.; Steiman, M. *Organometallics* **1994**, *13*, 647.
- (21) Guerra, G.; Cavallo, L.; Moscardi, G.; Vacatello, M.; Corradini, P. *J. Am. Chem. Soc.* **1994**, *116*, 2988.
- (22) Zambelli, A.; Sacchi, M. C.; Locatelli, P.; Zannoni, G. *Macromolecules* **1982**, *15*, 211.
- (23) Longo, P.; Grassi, A.; Pellicchia, C.; Zambelli, A. *Macromolecules* **1987**, *20*, 1015.
- (24) Hortmann, K.; Brintzinger, H. H. *New J. Chem.* **1992**, *16*, 51.
- (25) Castonguay, L. A.; Rappe', A. K. *J. Am. Chem. Soc.* **1992**, *114*, 5832.
- (26) Kuribayashi, K.; Koga, N.; Morokuma, K. *J. Am. Chem. Soc.* **1992**, *114*, 2359, 8687.
- (27) Hart, J. R.; Rappe', A. K. *J. Am. Chem. Soc.* **1993**, *114*, 6159.
- (28) Eksterowicz, J. E.; Houk, K. N. *Chem. Rev.* **1993**, *93*, 2439.
- (29) Corey, E. J.; Bailer, J. C., Jr. *J. Am. Chem. Soc.* **1959**, *81*, 2620.
- (30) (a) Schafer, A.; Karl, E.; Zsolnai, L.; Huttner, G.; Brintzinger, H. H. *J. Organomet. Chem.* **1987**, *328*, 87. (b) Brintzinger, H. H. In *Transition Metals and Organometallics as Catalysts for Olefin Polymerization*; Kaminsky, W., Sinn, H. J., Eds.; Springer Verlag: Berlin, 1988.
- (31) Hanson, K. R. *J. Am. Chem. Soc.* **1966**, *88*, 2731.
- (32) (a) Cahn, R. S.; Ingold, C.; Prelog, V. *Angew. Chem., Int. Ed. Engl.* **1966**, *5*, 385. (b) Prelog, V.; Helmchen, G. *Angew. Chem., Int. Ed. Engl.* **1982**, *21*, 567.
- (33) Schlögl, K. *Top. Stereochem.* **1966**, *1*, 39.
- (34) Stanley, K.; Baird, M. C. *J. Am. Chem. Soc.* **1975**, *97*, 6598.
- (35) Cossee, P. *Tetrahedron Lett.* **1960**, *17*, 12, 17.
- (36) (a) Hine, J. *J. Org. Chem.* **1966**, *31*, 1236. (b) Hine, J. *Adv. Phys. Org. Chem.* **1977**, *15*, 1.
- (37) (a) Venditto, V.; Guerra, G.; Corradini, P.; Fusco, R. *Polymer* **1990**, *31*, 530. (b) Venditto, V.; Guerra, G.; Corradini, P.; Fusco, R. *Eur. Polym. J.* **1991**, *27*, 45.
- (38) (a) Kraudelat, H.; Brintzinger, H. H. *Angew. Chem., Int. Ed. Engl.* **1990**, *29*, 1412. (b) Brintzinger, H. H.; Fischer, D.; Mülhaupt, R.; Rieger, B.; Waymouth, R. M. *Angew. Chem., Int. Ed. Engl.* **1995**, *34*, 1143.
- (39) Piers, W. E.; Bercaw, J. E. *J. Am. Chem. Soc.* **1990**, *112*, 9406.
- (40) Clawson, L.; Soto, J.; Buchwald, S. L.; Steigerwald, M. L.; Grubbs, R. H. *J. Am. Chem. Soc.* **1985**, *107*, 3377.
- (41) Suter, U. W.; Flory, P. J. *Macromolecules* **1975**, *8*, 765.
- (42) Doman, T. N.; Hollis, T. K.; Bosnich, B. *J. Am. Chem. Soc.* **1995**, *117*, 1352.
- (43) Mayo, S. L.; Olafson, B. D.; Goddard, W. A., III. *J. Phys. Chem.* **1990**, *94*, 8897.
- (44) Petraccone, V.; Pirozzi, B.; Frasci, A.; Corradini, P. *Eur. Polym. J.* **1976**, *12*, 323.
- (45) Ooi, T.; Scott, R. A.; Vandekooi, K.; Scheraga, H. A. *J. Chem. Phys.* **1967**, *46*, 4410.
- (46) Brooks, B. R.; Brucoleri, R. E.; Olafson, B. D.; States, D. J.; Swaminathan, S.; Karplus, M. *J. Comput. Chem.* **1983**, *4*, 187.
- (47) (a) Howeler, U.; Mohr, R.; Knickmeier, M.; Erker, G. *Organometallics* **1994**, *13*, 2380. (b) Cornell, W. D.; Cieplak, P.; Bayly, C. I.; Gould, I. R.; Kenneth, M. M., Jr.; Ferguson, D. M.; Spellmeyer, D. C.; Fox, T.; Caldwell, J. W.; Kollman, P. A. *J. Am. Chem. Soc.* **1995**, *117*, 5179.
- (48) (a) Corradini, P.; Barone, V.; Fusco, R.; Guerra, G. *Eur. Polym. J.* **1979**, *15*, 1133. (b) Dwyer, M.; Searle, G. A. *J. Chem. Soc., Chem. Commun.* **1972**, 726.
- (49) Niketic, M.; Rasmussen, K.; Waldluye, F.; Lifson, S. *Acta Chem. Scand.* **1976**, *A30*, 485.
- (50) Collins, S.; Gauthier, W. J.; Holden, D. A.; Kuntz, B. A.; Taylor, N. J.; Ward, D. G. *Organometallics* **1991**, *10*, 2061.
- (51) Cohen, S. A.; Auburn, P. R.; Bercaw, J. E. *J. Am. Chem. Soc.* **1983**, *105*, 1136.
- (52) (a) Jordan, R.; Bajgur, C.; Willet, R.; Scott, B. J. *Am. Chem. Soc.* **1986**, *108*, 7410. (b) Hlatky, G.; Turner, H.; Eckman, R. *J. Am. Chem. Soc.* **1989**, *111*, 2728. (c) Amorose, D. M.; Lee, R. A.; Petersen, J. L. *Organometallics* **1991**, *10*, 2191. (d) Horton, A.; Orpen, G. A. *Organometallics* **1991**, *10*, 3910. (e) Jordan, R. F.; LaPointe, R. E.; Bradley, P. K.; Baezinger, N. C. *Organometallics* **1989**, *8*, 2892. (f) Jordan, R. F.; Taylor, D. F.; Baezinger, N. C. *Organometallics* **1990**, *9*, 1546. (g) Jordan, R. F.; Taylor, D. F.; Baezinger, N. C. *Organometallics* **1987**, *6*, 1041. (h) Jordan, R. F.; Bradley, P. K.; Baezinger, N. C. *J. Am. Chem. Soc.* **1990**, *112*, 1289.
- (53) Woo, T. K.; Fan, L.; Ziegler, T. *Organometallics* **1994**, *13*, 432.
- (54) Mallin, D. T.; Rausch, M. D.; Lin, Y. G.; Dong, S.; Chien, J. C. W. *J. Am. Chem. Soc.* **1990**, *112*, 2030.
- (55) Mallin, D. T.; Rausch, M. D.; Lin, Y. G.; Winter, H. H.; Chien, J. C. W. *Macromolecules* **1992**, *25*, 1242.
- (56) Kibino, N.; Monoi, T.; Ohira, H.; Inazawa, S. *Eur. Pat. Appl.* **1992**, *544*, 308.
- (57) Giardello, M. A.; Eisen, M. S.; Stern, C. L.; Marks, T. J. *J. Am. Chem. Soc.* **1993**, *115*, 3326.
- (58) Ewen, J. A.; Elder, M. J. *Eur. Pat. Appl.* **1993**, *537*, 130.
- (59) Ewen, J. A.; Elder, M. J. In *Ziegler Catalysts*; Fink, G., Mülhaupt, R., Brintzinger, H. H., Eds.; Springer-Verlag: Berlin, 1995; p 99.
- (60) Miyake, S.; Okamura, Y.; Inazawa, S. *Macromolecules* **1995**, *28*, 3074.
- (61) Kaminsky, W.; Razavi, A. Oral presentations at the STE-POL'94, Milano, Italy, June 6–10, 1994.